

In Situ Synthesis of MOF Membranes on ZnAl-CO₃ LDH Buffer Layer-Modified Substrates

Yi Liu,^{*,†} Nanyi Wang,[†] Jia Hong Pan,[‡] Frank Steinbach,[†] and Jürgen Caro^{*,†}

[†]Department of Physical Chemistry and Electrochemistry, Leibniz University Hannover, Callinstr. 22, 30167, Hannover, Germany

[‡]Department of Materials Science and Engineering, National University of Singapore, 5 Engineering Drive 2, 117579, Singapore

S Supporting Information

ABSTRACT: We develop here a urea hydrolysis method to *in situ* prepare asymmetric ZnAl-CO₃ layered double hydroxide (LDH) buffer layers with various stable equilibrium morphology on porous Al₂O₃ substrates. In particular it is found that well-intergrown ZIF-8 membranes can be directly synthesized on the ZnAl-CO₃ LDH buffer layer-modified substrates, owing to the specific metal–imidazole interaction between ZnAl-CO₃ LDHs and ZIF-8. Other Zn-based MOF membranes, like ZIF-7 and ZIF-90, can also be synthesized with this method. Our finding demonstrates that LDH buffer layer represents a new concept for substrate modification.

Metal–organic framework (MOF) membranes are gaining widespread scientific attention due to their great potential for efficient separation of industrially important gas and liquid mixtures.¹ Although rapid progress has been made during the past years,² *in situ* growth of well-intergrown MOF membranes on porous ceramic substrates is still a challenge,³ owing to the low affinity interaction between MOF grains and the substrate. Therefore, surface modification of the substrate with reactive organic functional groups is often employed to assist the direct MOF crystallization. For instance, through the coordination effect between 3-aminopropylsilyl groups of 3-aminopropyltriethoxysilane and the free Zn²⁺ centers of ZIF nanocrystals, our group has developed a series of H₂-selective ZIF membranes, including ZIF-22,⁴ ZIF-90,⁵ and ZIF-95.⁶ Very recently, polydopamine modification was proven to be a powerful platform for covalent synthesis of MOF membranes.⁷ Besides, a novel counter-diffusion concept was developed in MOF membrane synthesis. With this method, well-intergrown HKUST-1⁸ and ZIF-8⁹ membranes were successively prepared and exhibited unprecedented gas selectivity.¹⁰ In particular, application of this technique for the growth of MOF layers on cheap organic hollow fibers^{2c,11} shows a bright prospect for the commercialization of MOF membranes in the future.

However, only little attention has been devoted to developing novel inorganic surface modifiers with unique advantages such as high affinity with the substrate, high thermal stability, no swelling, and eco-friendly and easy fabrication. Jeong, Lai et al. discovered that the nucleation and growth of MOF-5 crystals were enhanced on graphite-coated anodized aluminum oxide or Al₂O₃-supported substrates under microwave irradiation, owing to the specific electric and dielectric properties.¹² Very recently Zhang et al. fabricated H₂-selective ZIF-8 membranes on α-Al₂O₃

tubular substrates modified with ZnO in form of nanorods or ultrathin layers.^{2e,13} These studies demonstrated the great potential of inorganic compounds in MOF membrane fabrication. Nevertheless, most of the current inorganic compounds used for substrate modification are not reactive enough for direct *in situ* crystallization of MOFs. An additional secondary growth step is thus obligatory to obtain well-intergrown MOF membranes. In order to compete with well-developed organic functionalization methods the inorganic buffer layer should have a high affinity to MOF crystals so that well-intergrown MOF membranes can be prepared in one step.

Recently Nair solvothermally deposited roughened “whisker-like” MgO_xH_y layered nanostructures on surface LTA and MFI zeolites.¹⁴ Due to the adsorption and entanglement of polymer chains in the whisker structure, adhesion between zeolites and the polymer phase was greatly enhanced and yielded zeolite-polymer mixed matrix membranes with significantly improved gas separation performance. Inspired by Nair’s work, here we demonstrate that surface modification of substrates with ZnAl-CO₃ layered double hydroxide (LDH) buffer layers enables to greatly enhance the heterogeneous nucleation of ZIF-8 crystals and results in the formation of well-intergrown ZIF-8 membranes (Figure 1). LDHs, which have the general formula [M_{1-x}²⁺M_x³⁺(OH)₂][Aⁿ⁻]_{x/n}·zH₂O (M²⁺, M³⁺, and Aⁿ⁻ represent di-, tri-valent metal ions and *n*-valent anions), are a representative of layered inorganic compounds.^{15,16} ZIF-8, a promising MOF material with commercial prospects, has intrigued extensive interest due to its extraordinary thermal and hydrothermal stability.¹⁷

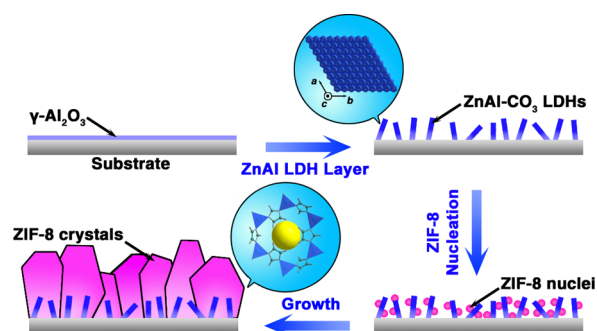
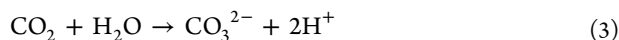
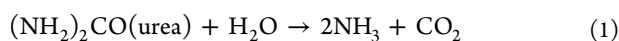


Figure 1. Schematic illustration of *in situ* solvothermal growth of ZIF-8 membrane on a ZnAl-LDH buffer layer-modified $\gamma\text{-Al}_2\text{O}_3$ substrate.

Received: July 21, 2014

Published: September 26, 2014

The ZnAl-CO₃ LDH layer was prepared via a facile chemical bath deposition method by immersing a porous γ -Al₂O₃ substrate in an aqueous precursor solution containing Zn(NO₃)₂·6H₂O and urea (details were shown in SI-1). Upon increasing the temperature, urea spontaneously hydrolyzes to NH₃ and CO₂ (eq 1). Owing to the excessive release of NH₃ and the low solubility of CO₂ in solution, hydrolysis of urea generates an alkaline medium favorable for heterogeneous nucleation of ZnAl-CO₃ LDH grains on the substrate (eq 2). Simultaneously CO₂ is converted to CO₃²⁻ and preferentially intercalated into the interlayer gallery (eq 3):¹⁸



Interestingly, the concentration of zinc ions [Zn²⁺] in the precursor solution was found to exert great influence on the resulting microstructure and crystal composition of ZnAl-CO₃ LDH buffer layers (Figures 2 and 3). In dilute solution ([Zn²⁺] =

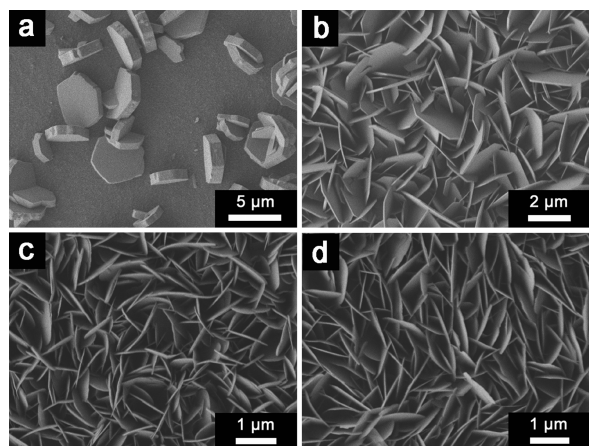


Figure 2. SEM images of ZnAl-CO₃ LDH layers prepared from the precursor solution with [Zn²⁺] concentrations of (a) 1.5×10^{-4} , (b) 2.3×10^{-4} , (c) 4.5×10^{-4} , and (d) 9×10^{-4} mol·L⁻¹. Reaction condition: 75 °C for 24 h.

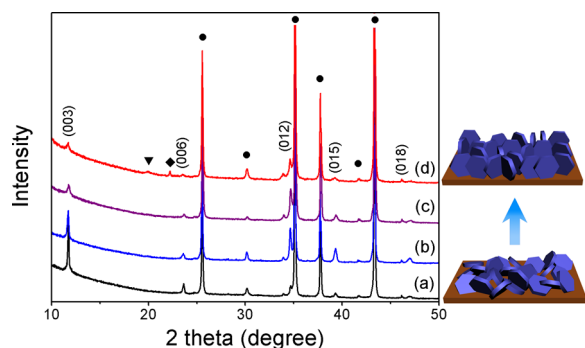


Figure 3. XRD patterns of ZnAl-CO₃ LDH layers prepared from the precursor solution with [Zn²⁺] concentrations of (a) 1.5×10^{-4} , (b) 2.3×10^{-4} , (c) 4.5×10^{-4} , and (d) 9×10^{-4} mol·L⁻¹. Reaction condition: 75 °C for 24 h. Diffractions derived from the substrate (●), ZnAl-NO₃ LDH (▼), and Zn₄(OH)₆CO₃·H₂O phase (◆) are marked.

1.5×10^{-4} mol·L⁻¹), LDH crystals were only sparsely grown on the substrate, and their average grain size (along the *a*-direction)

reached $\sim 5 \mu\text{m}$ (Figure 2a). Increasing the [Zn²⁺] to 2.3×10^{-4} mol·L⁻¹ led to formation of a uniform LDH layer with a reduced grain size ($\sim 3 \mu\text{m}$, Figure 2b) and thickness ($\sim 0.2 \mu\text{m}$, along the *c*-direction). Further increasing [Zn²⁺] to 4.5×10^{-4} and 9×10^{-4} mol·L⁻¹ resulted in a dramatic decrease of their grain size ($\sim 1 \mu\text{m}$) and thickness (~ 50 nm, Figure 2c,d). In addition, thickness of the LDH buffer layer was reduced from 3 to $0.8 \mu\text{m}$ with the increase of [Zn²⁺] (shown in SI-2). XRD patterns of all these LDH layers showed three conspicuous diffraction peaks at 2θ values of 11.7°, 23.5°, and 34.6°, which could be assigned to reflections of (003), (006), and (012) crystal planes of the ZnAl-CO₃ LDH phase (Figure 3).¹⁹ It is well-known that the $d_{(003)}$ -spacing equals to the basal spacing of LDH materials.²⁰ In this study, the (003) diffraction peaks of all the LDH layers appeared at 2θ value of 11.7°, which corresponded to a basal spacing of 0.75 nm according to the Bragg equation. This value coincided well with values for CO₃²⁻-intercalated LDH materials.²⁰

Selection of suitable substrates seems to be critical to the formation of ZnAl LDH layers. For comparison, we tried to grow *in situ* the ZnAl-CO₃ LDH buffer layer on a bare α -Al₂O₃ substrate. Nevertheless, almost no LDH crystals were attached to the substrate (shown in SI-3). This result is consistent with the finding by Duan et al. that upon urea hydrolysis ZnAl LDHs are prone to nucleate in bulk solution rather than on the substrate.^{15b,21} To facilitate the heterogeneous nucleation of ZnAl-CO₃ LDHs on the substrate, porous γ -Al₂O₃ substrates were used in our study, and accordingly uniform ZnAl-CO₃ LDH buffer layers with diverse microstructures were formed on the substrates. Presumably, compared with α -Al₂O₃, the γ -Al₂O₃ substrate is chemically more reactive and shows distinctive competence as the Al³⁺ source.²² Moreover, under this condition ZnAl-CO₃ LDHs preferentially nucleate and grow at the solution–substrate interface where both the Ni²⁺ and Al³⁺ are abundant. To the best of our knowledge, this is the first report of *in situ* growth of ZnAl-CO₃ LDH films by urea hydrolysis method. It was noted that besides urea route, ZnAl-NO₃ LDH layers could also form on porous γ -Al₂O₃ substrates with the “ammonia-assisted crystallization” method.²³ However, they are not qualified as buffer layers since underlying substrate pores are blocked by ZnAl-NO₃ LDH layers (shown in SI-4) even though the synthetic parameter is optimized.²⁴

For the successful application of ZnAl-CO₃ LDHs as buffer layers, one critical issue is the LDH crystal orientation control. Under ideal conditions LDH grains should arrange perpendicularly to the substrate surface to minimize the mass transfer resistance. In other words, an *ab*-oriented ZnAl-CO₃ LDH buffer layer is preferred. To quantify the preferred orientation of LDH layers, we define $I_r = I_{(012)}/I_{(003)}$, where $I_{(012)}$ and $I_{(003)}$ represent the peak heights of (012) and (003) diffractions, respectively. Higher I_r value indicates that more LDHs arrange with their *ab*-face (the largest face) perpendicular to the substrate. It was found that with the increase of [Zn²⁺] concentration, the I_r value first drastically increased from 0.19 to 1.20, reached the maximum (3.05), then decreased (2.54, shown in Figure 4). The preferred *ab*-orientation of the ZnAl-CO₃ LDH buffer layer can be interpreted by “evolution selection” mechanism.²⁵ During hydrothermal process, primary LDH nuclei with anisotropic nature show much faster growth rate along the *ab*-direction than along the *c*-direction. When two LDH crystals encounter, the more steeply growing crystal will inhibit the further evolution of the less steeply one. As a result, LDH grains tend to arrange with the *ab*-face perpendicular to the substrate.²⁶ Since adjacent LDH crystals are more tightly arranged with increasing [Zn²⁺]

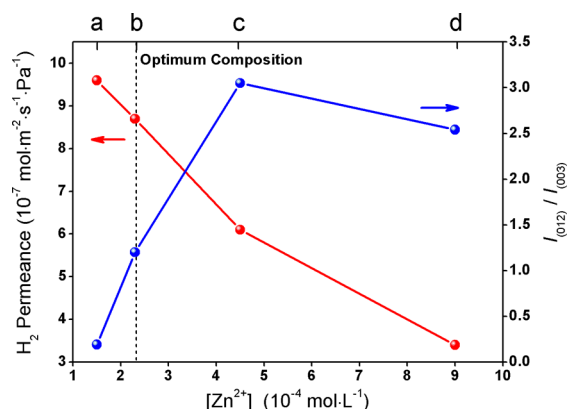


Figure 4. Dependence of the H₂ permeance and LDH crystal orientation parameter I_r of ZnAl-CO₃ LDH buffer layers on the [Zn²⁺] concentration in the precursor solution. The [Zn²⁺] concentration was (a) 1.5×10^{-4} , (b) 2.3×10^{-4} , (c) 4.5×10^{-4} , and (d) 9×10^{-4} mol·L⁻¹. Permeance was measured at $\Delta P = 1$ bar, $T = 25$ °C.

concentration (Figure 2), the “evolution selection” effect becomes dominant and results in the increase of I_r (insets of Figure 3). However, further increasing [Zn²⁺] to 9×10^{-4} mol·L⁻¹ leads to the formation of impure phases like zinc carbonate hydroxide hydrate and ZnAl-NO₃ LDHs, which may contribute to the slightly reduced I_r (2.54). Besides, it was noted that the (003) diffraction peak of the ZnAl-CO₃ LDH buffer layer synthesized from the lowest [Zn²⁺] concentration was much stronger and sharper (Figure 2a) than the materials obtained at higher [Zn²⁺] concentrations, which could be attributed to the remarkably improved crystallinity and the lower I_r value.

The interlayer space of ZnAl-CO₃ LDHs is still fully occupied with solvent molecules (H₂O) after *in situ* hydrothermal growth, thus precluding the possibility that H₂ could permeate through the LDH buffer layer via interlayer gallery at room temperature. The mass transfer resistance from the LDH buffer layer is then evaluated by comparing volumetric flow rates of single H₂ gas through various ZnAl-CO₃ LDH-modified Al₂O₃ substrates. It was found that the H₂ permeance was reduced from 9.6×10^{-7} to 3.4×10^{-7} mol·m⁻²·s⁻¹·Pa⁻¹ with the increase of [Zn²⁺] concentration (shown in Figure 4). This is because increasing the [Zn²⁺] concentration will lead to higher nucleation of LDH crystallites on the substrate. As a result, the mass transfer resistance will also increase. In comparison, the ZnAl-CO₃ LDH buffer layer with a [Zn²⁺] of 2.3×10^{-4} mol·L⁻¹ showed optimum microstructures for the growth of MOF membranes due to a uniform distribution of ZnAl-CO₃ LDH grains on the substrate, a preferred *ab*-orientation and a relatively low mass transfer resistance after the modification (H₂ permeance was 1.2×10^{-6} mol·m⁻²·s⁻¹·Pa⁻¹ on the bare substrate).

ZnAl-CO₃ LDHs is a promising candidate for surface modification since Zn²⁺ ions in the brucite-like sheets can provide active sites for the nucleation of ZIF-8 crystals. Moreover, the high length-to-width of ZnAl-CO₃ LDH grains further facilitates the nucleation and growth of MOF crystals on the substrate by guaranteeing a sufficient contact with the ZIF-8 precursor solution. In the next step, the LDH layer-modified substrate was immersed into diluted ZIF-8 precursor solution. After solvothermal growth, a compact and well-intergrown ZIF-8 layer with a thickness of ~ 20 μm was formed (shown in Figure 5a,b). The XRD pattern showed that these new emerging diffraction peaks matched well with the reported standard diffraction pattern of ZIF-8 powders (SI-5) so that the layer

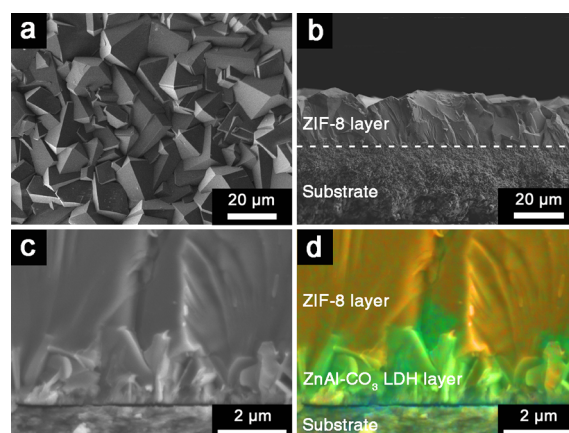


Figure 5. SEM images of the (a) top and (b) cross-sectional view of prepared ZIF-8 membrane. (c,d) SEM and EDXS mapping of the magnified cross-section of the supported ZIF-8 membrane. Color code: yellow = N; green = Al. Surface morphology of the LDH buffer layer used here is shown in Figure 2b.

indeed belonged to ZIF-8 phase. Energy-dispersive X-ray spectroscopy (EDXS) of the cross-section of ZIF-8 layer further confirmed that the ZnAl-CO₃ LDH phase located between the ZIF-8 layer and substrate (Figure 5c,d). It should be noted that for the formation of well-intergrown ZIF-8 membranes, the precursor solution should be aged before solvothermal reaction (SI-6).

To evaluate gas permeability of the membrane, volumetric flow rates of both single and mixed gases through the membrane were measured (details are shown in SI-7) and results are summarized in SI-8. The separation factor (SF) of the equimolecular H₂/CO₂, H₂/N₂, and H₂/CH₄ gas pairs reached 4.2, 10.0, and 12.5, respectively, with a H₂ permeance of 1.4×10^{-7} mol·m⁻²·s⁻¹·Pa⁻¹. In particular, the H₂/CH₄ SF of the membrane is comparable with the SF reported for high-quality ZIF-8 membranes, although the H₂ permeance is lower when compared with some thin (~ 2 μm) or hollow-fiber supported ZIF-8 membranes²⁷ (an exhaustive comparison with the literature is shown in Table S1). It should be emphasized that due to the framework flexibility ZIF-8, molecules with a kinetic diameter larger than the pore size of ZIF-8 (0.34 nm) like CH₄ (0.38 nm) could also pass through the membrane.²⁸ In addition, since the H₂ permeance sharply decreased to 1.4×10^{-7} mol·m⁻²·s⁻¹·Pa⁻¹ in case the ZIF-8 layer was *in situ* grown on the ZnAl-CO₃ LDH-modified Al₂O₃ substrate, we deduced that the mass transfer barrier was mainly derived from the ZIF-8 layer.

Very recently Eddaoudi developed a novel liquid-phase epitaxy method for preparation of ultrathin, continuous, and defect-free ZIF-8 membranes on a porous alumina substrate.²⁹ Permeation behaviors of a series of gas pairs were studied using the time lag technique. High H₂/CO₂ (~ 5), H₂/N₂ (~ 11), H₂/CH₄ (~ 12), and H₂/C₃H₈ (~ 60) selectivities are achieved. In particular authors reported for the first time unprecedented findings in relation to mixed CH₄/*n*-C₄H₁₀ gas separation through the ZIF-8 membrane. In comparison, the ZIF-8 membrane synthesized in the current study showed similar H₂/CO₂, H₂/N₂ and H₂/CH₄ selectivities, while the gas permeances were 1 order of magnitude higher than the former. Moreover, our study also revealed that the gas permeability slightly varied with time so that continuous measurements were required before the attainment of the steady state (typically 2 h is required).

We also tried *in situ* growth of ZIF-8 membrane on a bare γ - Al_2O_3 substrate. Nevertheless, ZIF-8 crystals were only sparsely attached to the substrate (SI-9). This comparative experiment confirmed the importance of ZnAl-CO_3 LDH buffer layer in promoting nucleation and growth of ZIF-8 crystals.

Our approach was not only confined to ZIF-8 membrane synthesis. For instance, both well-intergrown ZIF-7 (shown in SI-10) and ZIF-90 (shown in SI-11) membranes could also grow on the ZnAl-CO_3 LDH buffer layer-modified Al_2O_3 substrates. In contrast, both ZIF-7 and ZIF-90 grains were only sparsely distributed on bare substrates.^{2c,30}

It should be noted that through physical interactions, recently we deposited ZIF-8 seeds on an α - Al_2O_3 substrate modified with a network of vertically aligned MgAl-CO_3 LDH walls.³¹ The LDH network effectively collected seeds in a “perch” and prevented ZIF-8 seeds from peeling off during secondary growth. In contrast, the present study reveals the inherent high affinity interaction between ZnAl-CO_3 LDHs and ZIF-8 crystals, which lead to the formation of well-intergrown ZIF-8 layers in one step. In addition, nucleation and growth kinetics of ZnAl-CO_3 and MgAl-CO_3 LDH films are also quite different.^{15b} This is the first report of *in situ* growth of ZnAl-CO_3 LDH films with urea hydrolysis method, whereas it is well-recognized that MgAl-CO_3 LDH films can be prepared by hydrolysis of urea.

In summary, a novel synthetic strategy has been developed for the *in situ* growth of ZnAl-CO_3 LDH buffer layers with diverse microstructures on porous γ - Al_2O_3 substrates via a urea hydrolysis method. The γ - Al_2O_3 phase on the substrate serves as the Al^{3+} source for the homogeneous nucleation and the subsequent growth of the LDH buffer layer. The resultant ZnAl-CO_3 LDH grains possess a high-affinity interaction with the ZIF-8 phase, leading to the formation of a well-intergrown ZIF-8 membrane in a dilute precursor solution. The developed approach is simple, green, effective, and cost-effective and can be applied to prepare other Zn-based MOF membranes.

■ ASSOCIATED CONTENT

● Supporting Information

Experimental procedures and characterization data. This material is available free of charge via the Internet at <http://pubs.acs.org>.

■ AUTHOR INFORMATION

Corresponding Authors

yi.liu@pci.uni-hannover.de

juergen.caro@pci.uni-hannover.de

Notes

The authors declare no competing financial interest.

■ ACKNOWLEDGMENTS

Y.L. is grateful for the financial support from Alexander von Humboldt Foundation. We acknowledge financial support by EU CARENA (FP7-NMP-2010-LARGE-4, Nr. 263007).

■ REFERENCES

- (1) (a) Zacher, D.; Shekha, O.; Wöll, C.; Fischer, R. A. *Chem. Soc. Rev.* **2009**, *38*, 1418. (b) Shekha, O.; Liu, J.; Fischer, R. A.; Wöll, C. *Chem. Soc. Rev.* **2011**, *40*, 1081. (c) Shah, M.; McCarthy, M. C.; Sachdeva, S.; Lee, A. K.; Jeong, H. K. *Ind. Eng. Chem. Res.* **2012**, *51*, 2179. (d) Gascon, J.; Kapteijn, F.; Zornoza, B.; Sebastian, V.; Casado, C.; Coronas, J. *Chem. Mater.* **2012**, *24*, 2829. (e) Yao, J. F.; Wang, H. T. *Chem. Soc. Rev.* **2014**, *43*, 4470.
- (2) (a) Bux, H.; Feldhoff, A.; Cravillon, J.; Wiebcke, M.; Li, Y. S.; Caro, J. *Chem. Mater.* **2011**, *23*, 2262. (b) Li, Y. S.; Liang, F. Y.; Bux, H.;

- Feldhoff, A.; Yang, W. S.; Caro, J. *Angew. Chem., Int. Ed.* **2010**, *49*, 548.
- (c) Brown, A. J.; Johnson, J. R.; Lydon, M. E.; Koros, W. J.; Jones, C. W.; Nair, S. *Angew. Chem., Int. Ed.* **2012**, *51*, 10615. (d) Pan, Y. C.; Lai, Z. P. *Chem. Commun.* **2011**, *47*, 10275. (e) Zhang, X. F.; Liu, Y. Q.; Kong, L. Y.; Liu, H. O.; Qiu, J. S.; Han, W.; Weng, L. T.; Yeung, K. L.; Zhu, W. D. *J. Mater. Chem. A* **2013**, *1*, 10635. (f) Dong, X. L.; Lin, Y. S. *Chem. Commun.* **2013**, *49*, 1196.
- (3) McCarthy, M. C.; Varela, V. V.; Barnett, G. V.; Jeong, H. K. *Langmuir* **2010**, *26*, 14636.
- (4) Huang, A. S.; Bux, H.; Steinbach, F.; Caro, J. *Angew. Chem., Int. Ed.* **2010**, *49*, 4958.
- (5) Huang, A. S.; Dou, W.; Caro, J. *J. Am. Chem. Soc.* **2010**, *132*, 15562.
- (6) Huang, A. S.; Chen, Y. F.; Wang, N. Y.; Hu, Z. Q.; Jiang, J. W.; Caro, J. *Chem. Commun.* **2012**, *48*, 10981.
- (7) Liu, Q.; Wang, N. Y.; Caro, J.; Huang, A. S. *J. Am. Chem. Soc.* **2013**, *135*, 17679.
- (8) Ameloot, R.; Vermoortele, F.; Vanhove, W.; Roeyfaers, M. B. J.; Sels, B. F.; De Vos, D. E. *Nat. Chem.* **2011**, *3*, 382.
- (9) Yao, J.; Dong, D.; Li, D.; He, L.; Xu, G.; Wang, H. *Chem. Commun.* **2011**, *47*, 2559.
- (10) Kwon, H. T.; Jeong, H. K. *J. Am. Chem. Soc.* **2013**, *135*, 10763.
- (11) Brown, A. J.; Brunelli, N. A.; Eum, K.; Rashidi, F.; Johnson, J. R.; Koros, W. J.; Jones, C. W.; Nair, S. *Science* **2014**, *345*, 72.
- (12) (a) Yoo, Y.; Jeong, H. K. *Chem. Commun.* **2008**, *44*, 2441. (b) Yoo, Y.; Lai, Z.; Jeong, H. K. *Microporous Mesoporous Mater.* **2009**, *123*, 100.
- (13) Zhang, X. F.; Liu, Y. G.; Li, S. H.; Kong, L. Y.; Liu, H. O.; Li, Y. S.; Han, W.; Yeung, K. L.; Zhu, W. D.; Yang, W. S.; Qiu, J. S. *Chem. Mater.* **2014**, *26*, 1975.
- (14) (a) Bae, T. H.; Liu, J. Q.; Lee, J. S.; Koros, W. J.; Jones, C. W.; Nair, S. *J. Am. Chem. Soc.* **2009**, *131*, 14662. (b) Lydon, M. E.; Unocic, K. A.; Bae, T. H.; Jones, C. W.; Nair, S. *J. Phys. Chem. C* **2012**, *116*, 9636.
- (15) (a) Zhao, M. Q.; Zhang, Q.; Huang, J. Q.; Wei, F. *Adv. Funct. Mater.* **2012**, *22*, 675. (b) Guo, X. X.; Zhang, F. Z.; Evans, D. G.; Duan, X. *Chem. Commun.* **2010**, *46*, 5197.
- (16) Wang, Q.; O'Hare, D. *Chem. Rev.* **2012**, *112*, 4124.
- (17) (a) Park, K. S.; Ni, Z.; Côté, A. P.; Choi, J. Y.; Huang, R. D.; Uribe-Romo, F. J.; Chae, H. K.; O'Keeffe, M.; Yaghi, O. M. *Proc. Natl. Acad. Sci. U.S.A.* **2006**, *103*, 10186. (b) Phan, A.; Doonan, C. J.; Uribe-Romo, F. J.; Knobler, C. B.; O'Keeffe, M.; Yaghi, O. M. *Acc. Chem. Res.* **2010**, *43*, 58.
- (18) Pan, J. H.; Zhang, X. W.; Du, A. J.; Bai, H. W.; Ng, J. W.; Sun, D. *Phys. Chem. Chem. Phys.* **2012**, *14*, 7481.
- (19) Liu, J. Q.; Song, J. Y.; Xiao, H. D.; Zhang, L. J.; Qin, Y. W.; Liu, D. H.; Hou, W. G.; Du, N. *Powder Technol.* **2014**, *253*, 41.
- (20) Wei, M.; Xu, X. Y.; Wang, X. R.; Li, F.; Zhang, H.; Lu, Y. L.; Pu, M.; Evans, D. G.; Duan, X. *Eur. J. Inorg. Chem.* **2006**, 2831.
- (21) Chen, H. Y.; Zhang, F. Z.; Chen, T.; Xu, S. L.; Evans, D. G.; Duan, X. *Chem. Eng. Sci.* **2009**, *64*, 2617.
- (22) Liu, Y.; Wang, N. Y.; Cao, Z. W.; Caro, J. *J. Mater. Chem. A* **2014**, *2*, 1235.
- (23) (a) Zhang, F. Z.; Zhao, L. L.; Chen, H. Y.; Xu, S. L.; Evans, D. G.; Duan, X. *Angew. Chem., Int. Ed.* **2008**, *47*, 2466. (b) Chen, H. Y.; Zhang, F. Z.; Duan, X. *Adv. Mater.* **2006**, *18*, 3089.
- (24) Liu, Y.; Wang, N. Y.; Caro, J. *J. Mater. Chem. A* **2014**, *2*, 5716.
- (25) van der Drift, A. *Philips Res. Rep.* **1967**, *22*, 267.
- (26) Guo, X. X.; Xu, S. L.; Zhao, L. L.; Lu, W.; Zhang, F. Z.; Evans, D. G.; Duan, X. *Langmuir* **2009**, *25*, 9894.
- (27) (a) Tao, K.; Cao, L. J.; Lin, Y. C.; Kong, C. L.; Chen, L. J. *J. Mater. Chem. A* **2013**, *1*, 13046. (b) Pan, Y. C.; Wang, B.; Lai, Z. P. *J. Membr. Sci.* **2012**, *421–422*, 292.
- (28) Fairen-Jimenez, D.; Moggach, S. A.; Wharmby, M. T.; Wright, P. A.; Parsons, S.; Düren, T. *J. Am. Chem. Soc.* **2011**, *133*, 8900.
- (29) Shekha, O.; Swaidan, R.; Belmabkhout, Y.; du Plessis, M.; Jacobs, T.; Barbour, L. J.; Pinnau, I.; Eddaoudi, M. *Chem. Commun.* **2014**, *50*, 2089.
- (30) Li, Y. S.; Bux, H.; Feldhoff, A.; Li, G. L.; Yang, W. S.; Caro, J. *Adv. Mater.* **2010**, *22*, 3322.
- (31) Liu, Y.; Wang, N. Y.; Diestel, L.; Steinbach, F.; Caro, J. *Chem. Commun.* **2014**, *50*, 4225.